Identification of a Consensus DNA-Binding Site for the *Arabidopsis thaliana* SBP Domain Transcription Factor, AtSPL14, and Binding Kinetics by Surface Plasmon Resonance[†]

Xinwen Liang, Tara J. Nazarenus, and Julie M. Stone*

Department of Biochemistry, Plant Science Initiative, Redox Biology Center, University of Nebraska, Lincoln, Nebraska 68588

Received July 20, 2007; Revised Manuscript Received January 8, 2008

ABSTRACT: Proteins with a conserved Cys- and His-rich SQUAMOSA promoter binding protein (SBP) domain are transcription factors restricted to photosynthetic organisms that possess a novel two Zn-finger structure DNA-binding domain. Despite the fact that altered expression of some SBP-encoding genes has profound effects on organism growth and development, little is known about SBP domain protein target genes. Misexpression of the *Arabidopsis thaliana AtSPL14* SBP domain gene confers resistance to programmed cell death and modifies plant architecture. A consensus DNA-binding motif for AtSPL14 was identified by systematic evolution of ligands by exponential enrichment (SELEX) or random binding site selection (RBSS). DNA recognized by AtSPL14 contained the core binding motif (GTAC) found for other SBP domain proteins, but mutational analyses indicated that at least one additional flanking nucleotide is necessary for effective AtSPL14−DNA interaction. Comparison of several SBP domain amino acid sequences allows us to hypothesize which specific amino acids might participate in this sequence-specific DNA recognition. Electrophoretic mobility shift assays (EMSA) with mutant AtSPL14 DNA-binding domain proteins indicated that not all of the Zn^{2+} ion coordinating ligands in the second Zn structure are strictly required for DNA binding. Surface plasmon resonance (SPR) was used to evaluate AtSPL14 *in vitro* binding kinetics for comparison of equilibrium binding constants with other SBP domain proteins. These data provide a strong basis for further experiments aimed at defining and distinguishing the sets of genes regulated by the closely related SBP domain family members.

Proper growth and development of multicellular organisms depend on a delicate balance between cell proliferation and programmed cell death (PCD).[1] In plants, PCD is required for tracheary element differentiation to form the water-conducting xylem tissue and accurate formation of various reproductive organs (*1*–*5*). PCD is also an important aspect of plant defense against pathogen attack (*6*–*8*). Despite the essential nature of PCD, large gaps remain in our knowledge of the mechanistic details and molecular components controlling plant PCD. Therefore, to identify novel genes that might participate in plant PCD, we developed a mutant selection scheme for the model plant *Arabidopsis thaliana* using a PCD-inducing fungal toxin fumonisin B1 (FB1), to identify FB1-resistant (*fbr*) mutants (*9*–*11*). Misexpression of the *AtSPL14* gene in the *fbr6* mutant confers the ability to proliferate in the presence of FB1 and modifies normal plant architecture, linking the insensitivity to cell death to altered plant development (*9*). AtSPL14 has features of a DNA-binding transcription factor, including a Cys- and His-rich SQUAMOSA promoter binding protein (SBP) domain predicted to bind DNA, ankyrin repeats that mediate protein–protein interactions, nuclear localization, and ability to bind to *A. thaliana* genomic DNA (*9*).

SBP domain proteins are defined by a conserved approximately 80 amino acid–protein domain (the SBP domain or SBP box) found only in proteins from photosynthetic organisms, ranging from single-celled algae (e.g., *Chlamydomonas reinhardtii*) to higher plants (e.g., *A. thaliana* and *Oryza sativa*). The SBP gene families are comprised of 16 genes in *A. thaliana* and 19 genes in *O. sativa* that encode proteins that share the highly conserved SBP DNA-binding domain but are diverse in overall domain structure (*12, 13*). To date, only a few functions for SBP domain proteins have been reported, perhaps due to genetic redundancy of closely related family members. In all cases, SBP domain proteins have been implicated in various aspects of plant growth and development, including metal sensing in algae and directing development of leaves, embryos, and floral organs in higher

[†] This research was supported by a grant from the Chemical Sciences, Geosciences and Biosciences Division, Office of Basic Energy Sciences, Office of Science, U.S. Department of Energy (DE-FG02-05ER15648) to J.M.S. and is a contribution of the Nebraska Agricultural Research Division.

* Address correspondence to this author. E-mail: jstone2@unl.edu. Phone: 402-472-4902. Fax: 402-472-3139.

[1] Abbreviations: CuRE, copper-responsive element; dsDNA, double-stranded DNA; DTT, dithiothreitol; EDTA, ethylenediaminetetraacetic acid; EMSA, electrophoretic mobility shift assay; FB1, fumonisin B1; *fbr*, FB1-resistant; HEPES, *N*-(2-hydroxyethyl)piperazine-*N*′-2-ethanesulfonic acid; IPTG, isopropyl β-D-1-thiogalactopyranoside; NMR, nuclear magnetic resonance; PCD, programmed cell death; PMSF, phenylmethanesulfonyl fluoride; RBSS, random binding site selection; RU, resonance (response) units; SA, streptavidin; SBP, SQUAMOSA promoter binding protein; SDS, sodium dodecyl sulfate; SELEX, systematic evolution of ligands by exponential enrichment; SPL, SQUAMOSA promoter binding protein-like; SPR, surface plasmon resonance; WT, wild type.

10.1021/bi701431y CCC: $40.75
Published on Web 02/27/2008

plants (*9, 13–22*). Some of these SBP domain proteins may also be posttranscriptionally regulated by noncoding microRNAs to control their spatial and temporal expression (*23–25*). Despite the obvious importance of these proteins, the specific genes targeted by individual SBP domain family members and the molecular consequences of their actions are largely unknown.

To fully understand the physiological functions of AtSPL14 in regulating plant PCD and/or development, AtSPL14 target genes, their modes of regulation, and the consequences of expression/repression need to be determined. As one step toward that goal, we used an affinity-based assay, referred to as systematic evolution of ligands by exponential enrichment (SELEX) or random binding site selection (RBSS) to screen a random pool of dsDNA fragments for sequences capable of binding to recombinant AtSPL14 protein. From this analysis, an AtSPL14-binding consensus DNA motif was derived. Mutational analyses indicated that predominantly the core motif, CGTAC, is essential for AtSPL14 protein binding to the DNA *in vitro*.

Recent structures of SBP domains determined by nuclear magnetic resonance (NMR) indicate that SBP domains form a unique two Zn-finger structure DNA-binding domain (*26, 27*). The SBP domain contains eight absolutely conserved Cys or His residues, some of which are critical for SBP domain DNA binding (*28*). We determined that all of the highly conserved cysteines in the two Zn^{2+} ion binding structures of the AtSPL14 SBP domain binding are important for DNA recognition by electrophoretic mobility shift assays (EMSA) and surface plasmon resonance (SPR). Yet, an AtSPL14 SBP domain with one of the Cys residues in the second Zn-finger structure mutated retained some DNA-binding ability. Moreover, we monitored the kinetic features of the AtSPL14 SBP domain−DNA binding by SPR. We further compare and contrast the target sequences and the equilibrium binding constants we determined for AtSPL14 with those of other SBP domain proteins (*18, 28, 29*).

MATERIALS AND METHODS

Recombinant AtSPL14 Protein Expression and Purification. Two different truncated and epitope-tagged versions of recombinant AtSPL14 proteins were used. The full-length AtSPL14 cDNA was generated by reverse transcription−polymerase chain reaction (RT-PCR) from RNA isolated from ecotype Col-0 (the reference genotype for the *A. thaliana* genome) using oligonucleotide primers SBPF (5′-GGATCCATGGATGAGGTAGGAGCTCAAGTG-3′) and SBPR (5′-ACTAGTCCGGATCCGATTGAGCCATAATCCAAACCTC-3′) and verified by DNA sequencing (*30*). Engineered *Bam*HI and existing internal *Sal*I restriction enzyme recognition sites were used to subclone FBR6 short (FBR6s; aa 1−402) into *Bam*HI/*Sal*I-digested pET-28a(+) to produce a protein composed of an N-terminal His tag, thrombin cleavage site, and T7 tag fused to a region of AtSPL14 encompassing the DNA-binding domain (Novagen, EMD Chemicals, Inc., Darmstadt, Germany). The His-tagged FBR6s protein was 447 amino acids with a predicted molecular mass of 48.8 kDa.

For electrophoretic mobility shift assays (EMSA) and surface plasmon resonance (SPR) binding assays, recombinant epitope-tagged FBR6 supershort (FBR6ss; aa 111–200) protein was used. The conserved SBP domain of AtSPL14 was amplified by PCR using oligonucleotide primers oJS86 (5′-CCGAATTCTCTCCGGGAGGGAATTATCCC-3′) and oJS87 (5′-CCGAATTCTTATGCAACCTCCTCCGGCTGCG-3′) and verified by DNA sequencing (*30*). The resulting PCR product was subcloned into pET-28a(+) to produce a protein composed of an N-terminal His tag, thrombin cleavage site, and T7 tag fused to a region of AtSPL14 encompassing the DNA-binding domain. The His-tagged FBR6ss protein was 126 amino acids with a predicted molecular mass of 14.3 kDa.

The recombinant proteins were expressed in *Escherichia coli* by inducing log phase cultures with 0.2 mM isopropyl β-D-1-thiogalactopyranoside (IPTG) at 37 °C for 2 h, and proteins were purified on Ni^{2+}-conjugated affinity resin according to the manufacturer's instructions (ProBond Purification System; Invitrogen, Carlsbad, CA). For SELEX experiments proteins were retained on the resin.

Site-Directed Mutagenesis. The site-directed mutagenesis was performed according to the Stratagene's QuickChange site-directed mutagenesis kit instruction manual (Stratagene, Cedar Creek, TX). Oligonucleotide primers used to mutate the nucleotides in the AtSPL14-binding DNA and the cysteine residues of the AtSPL14 SBP domain are shown in Tables S1 and S2 of the Supporting Information, respectively.

Systematic Evolution of Ligands by Exponential Enrichment (SELEX) or Random Binding Site Selection (RBSS). A random pool of oligonucleotides (76 nucleotides) of sequence 5′-GCTGCAGTTGCACTGAATTCGCCTCN$_{26}$CGACAGGATCCGCTGAACTGACCTG-3′, where N_{26} represents 26 randomized nucleotides, was synthesized by equimolar incorporation of A, G, C, and T at each "N" position (Integrated DNA Technologies, Coralville, IA). The two sets of 25 nucleotides flanking the 26-nucleotide random core were designed for amplification by PCR. To make double-stranded DNA (dsDNA), the random pool of oligonucleotides (100 ng) was subjected to PCR using the forward primer and Taq polymerase enzyme (94, 68, and 72 °C, 1 cycle), and the PCR products were purified by agarose gel electrophoresis (1.5% MetaPhor agarose; Cambrex Bio Science Rockland, Inc., Rockland, ME) to yield ds-R76, the substrate in the initial binding reaction.

The binding reactions were carried out on ice essentially as described with a few modifications (*31*). The recombinant protein T7-His$_6$-FBR6s was purified using a His tag purification kit (ProBond; Invitrogen, Carlsbad, CA) and retained on the resin. The resin with immobilized protein (200 μL) was washed twice with binding buffer (20 mM Tris-HCl, pH 7.6, 50 mM NaCl, 1 mM $MgCl_2$, 0.2 mM EDTA, 5% glycerol, 0.5 mM DTT, 50 μM PMSF), mixed with 50 μg/mL poly(dIdC) (Amersham Biosciences, Cleveland, OH) to reduce nonspecific binding for 10 min, and incubated with ds-R76 DNA (200 ng) for 60 min, with gentle tapping every 10 min. The immobilized protein−DNA complexes were washed with TN buffer (10 mM Tris-HCl, pH 7.4, 150 mM NaCl) five times, and the DNA was eluted with 200 μL of dissociation buffer (0.5 M Tris-HCl, pH 7.4, 20 mM EDTA, 10 mM NaCl, 0.2% SDS). The bound DNA was amplified by PCR using 250 nM oligonucleotide primers that anneal to the defined terminal sequences of the 76-nucleotide oligonucleotide for 20 cycles. The resulting product was used as the substrate in the second round of SELEX. After five

serial selection rounds, the amplified DNA was cloned into vector pGEM-TEasy (Promega, Madison, WI) and subjected to DNA sequencing (University of Nebraska−Lincoln, Genomics Core Facility). Effective DNA binding was verified by electrophoretic mobility shift assay (EMSA) competition assays.

Electrophoretic Mobility Shift Assay (EMSA). DNA fragments were fluorescently labeled by PCR amplification in a reaction containing 100 μM dNTPs, 1× PCR buffer, 1.5 mM $MgCl_2$, 2 ng of DNA template (pGEM-TEasy subclones selected from SELEX), 300 nM 5′-IR-dye 700 GTACCTTCGTTGCCGCTAG-3′ corresponding to the T7 promoter (Li-Cor, Lincoln, NE), 300 nM primer R or primer F, and Taq polymerase enzyme. The resulting PCR product was quantified using gel electrophoresis. Electrophoretic mobility shift assay binding reactions were performed in the same binding buffer used in the SELEX (exception: 1 mM DTT and no PMSF) in a total volume of 20 μL containing 60 nM protein and 4 nM labeled DNA and incubated for 30 min at 25 °C in darkness prior to electrophoresis. The protein−DNA binding mixture was electrophoretically resolved for 45 min at 4 °C in the dark on a prerun 8% nondenaturing polyacrylamide gel (polyacrylamide-bis ratio = 37.5:1) in Tris−borate−EDTA buffer (89 mM Tris, 89 mM boric acid, and 2.5 mM EDTA) at constant voltage (15 V/cm). Gels were analyzed using an Odyssey Infrared Imager (Li-Cor, Lincoln, NE).

Immobilization of Biotinylated DNA on the SA Sensor Chip. Cognate and noncognate DNA fragments (156 bp) containing dsR76 used in the SELEX experiments were biotinylated by PCR amplification with dsDNA cloned in pGEM-TEasy as templates, 5′-biotin-GTACCTTCGTTGCCGCTAG-3′ oligonucleotide corresponding to the T7 promoter (IDTDNA, Cedar Rapids, IA), and either primer R or primer F. The PCR products were purified by the QIAquick PCR purification kit (Qiagen, Valencia, CA), and DNA was immobilized on streptavidin (SA) sensor chips (Biacore AB, Uppsala, Sweden).

5′-Biotin-labeled DNA (the random binding site selected DNA 14 containing the consensus FBR6ss binding site, CCGTAC, Figure 1) was immobilized onto the SA sensor chip surface [450 resonance (response) units, RU] to provide the maximal level of RU associated with protein binding in the range of 50–100 RU. SA chips were conditioned with three consecutive 1 min injections of 1 M NaCl and 50 mM NaOH prior to immobilization. Two reference cells were used as controls for background subtraction: reference 1 was the surface alone (no bound DNA), and reference 2 had a noncognate DNA (a random DNA that did not possess the consensus binding motif) immobilized to the reference cell at the same concentration as the cognate DNA.

Surface Plasmon Resonance (SPR) Analysis. The purified His-FBR6ss protein was desalted and equilibrated in HBS-EP buffer using Centricon-mediated centrifugal filtration (10 kDa cutoff; Millipore, Billerica, MA). The protein was diluted in HBS-EP buffer to yield several different concentrations ranging from 3.25 to 300 nM. Varying protein concentrations were injected at a 75 μL/min flow rate. The chip surface was regenerated by injection of 0.1% SDS and 3 mM EDTA buffer for 1 min after each protein injection. Responses from the reference cell(s) were subtracted to correct for refractive index changes and nonspecific binding.

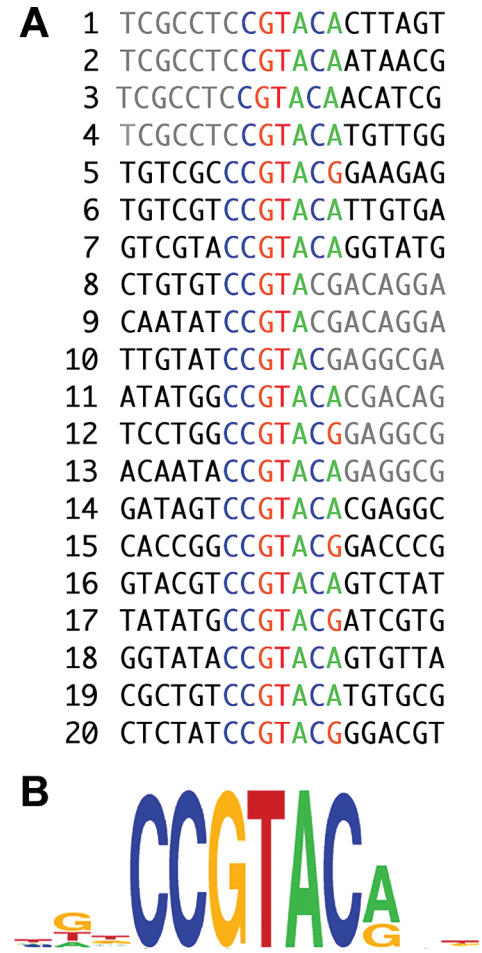

FIGURE 1: The consensus target site for the AtSPL14 SBP DNA-binding domain determined by SELEX. Double-stranded DNA molecules containing a 26-nucleotide completely randomized central region were subjected to repetitive cycles of binding to recombinant AtSPL14 bound to a Ni^{2+}-chelating affinity resin and PCR amplification. The individual binders were subsequently tested by electrophoretic mobility shift assays (EMSA) and competition with unlabeled probe (as in Figure 2A), yielding 20 distinct dsDNA fragments capable of binding to the AtSPL14 SBP domain. (A) An alignment of the 20 individual binders based on the results of the web-based multiple expectation maximization for motif elicitation (MEME) analysis program (*36*). The core consensus sequence nucleotides are in color, the adjacent random nucleotides are in black, and the nonrandom nucleotides derived from the fixed sequence immediately flanking the random nucleotides in the dsDNA pool are in gray. (B) A representation of the consensus DNA target binding motif (disregarding the fixed nucleotides flanking the random core) using WebLogo (*37*). The degree of conservation is indicated by the height of the letters. The core sequence "CCGTAC" was found in all dsDNA-binding fragments.

SPR Data Analysis. Data were analyzed with BIAevaluation 3.0 software (Biacore, Piscataway, NJ), which automatically calculates binding parameters taking into account control and experimental results allowing for quantitative kinetic analyses. Association (k_a) and dissociation (k_d) rates and overall affinity, the equilibrium dissociation constant (K_D), were calculated using a simple bimolecular 1:1 Langmuir isotherm binding model (A + B ↔ A−B) and a mass transfer model that accounts for mass transfer limitations due to rapid association and/or dissociation rates (*32*). Nonspecific binding effects were subtracted using the sensorgram generated from the control reference cell(s). Experiments were replicated in triplicate with similar results.

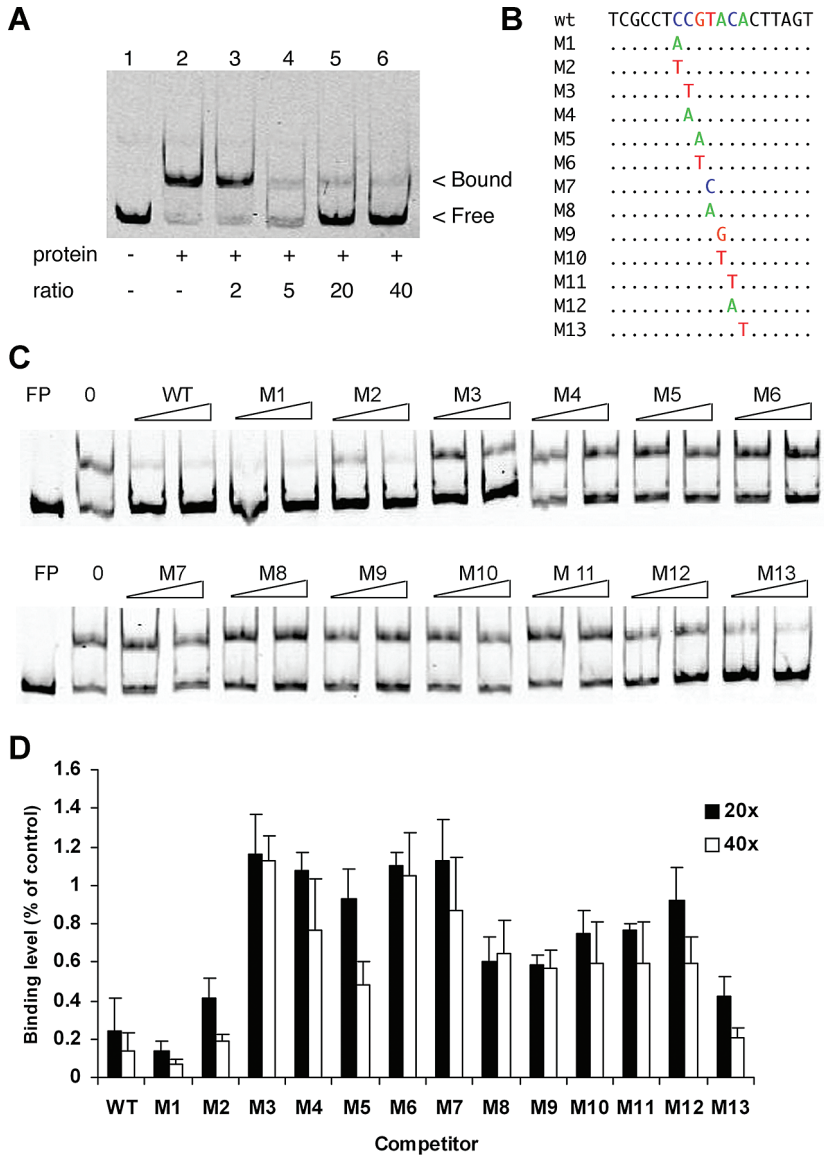

FIGURE 2: Specific AtSPL14 DNA binding by electrophoretic mobility shift assays (EMSA) and competition assays. (A) An example of the initial competition assays by EMSA used to determine binding of the individual dsDNA fragments identified by SELEX. The double-stranded DNA probe was generated by PCR with IRDye 700 fluorescently labeled (probe) or unlabeled (competitor) oligonucleotide primers. The probe (4 nM) was incubated without (−) or with (+) recombinant His-tagged AtSPL14 SBP domain protein (FBR6ss, 60 nM). For testing specificity, increasing amounts of unlabeled competitor were included in the binding reaction; the ratio of competitor:probe is indicated. "Complexes" were separated on an 8% nondenaturing polyacrylamide gel and visualized by infrared imaging. Lanes: (1) free probe; (2) probe plus AtSPL14 SBP domain protein; (3–6) probe plus increasing amounts of unlabeled competitor. (B) For EMSA competition assays, single nucleotide substitutions in the core consensus binding site of a selected dsDNA-binding fragment were generated by site-directed mutagenesis. The core consensus motif is in color with flanking nucleotides in black for the wild-type (wt) dsDNA, and individual nucleotide changes for the mutated (M1–M13) dsDNA are indicated. (C) EMSA competition assays with the wild-type (WT) or mutated (M1–M13) dsDNA fragments. For the binding reactions, "FP" indicates free probe with no protein, "0" indicates no competitor, and the triangles represent increasing amount of competitor in the binding reaction (20× or 40× molar ratios). (D) Band intensities corresponding to bound complexes were determined by infrared imaging (Odyssey; Li-Cor, Lincoln, NE). Binding efficiencies were normalized to a control binding reaction with no competitor on each gel ("0" in panel C). Binding levels with a 20× molar ratio (black bars) and a 40× molar ratio (white bars) of unlabeled competitor are shown. Error bars represent 95% confidence levels from experiments performed in triplicate.

RESULTS

Identification of a Consensus Binding Site for the AtSPL14 SBP Domain by Systematic Evolution of Ligands by Exponential Enrichment (SELEX). SELEX or random binding site selection (RBSS), an *in vitro* oligonucleotide binding and PCR amplification method, was used to define consensus DNA-binding sequences for the AtSPL14 SBP DNA-binding domain (*33–35*). The AtSPL14-binding DNA was selected from a pool of 76 bp of double-stranded DNA (dsDNA) with a central core of 26 random nucleotides by repeated cycles of binding to the hexahistidine-tagged FBR6s protein (encompassing the SBP DNA-binding domain) immobilized on Ni^{2+}-chelating affinity resin. Fifty-seven individual clones that were derived from five serial rounds of selection were subcloned and subjected to DNA sequencing, revealing that identical clones were identified multiple times. All of the unique clones were tested for binding to FBR6ss using EMSA assays and competition with unlabeled dsDNA probe.

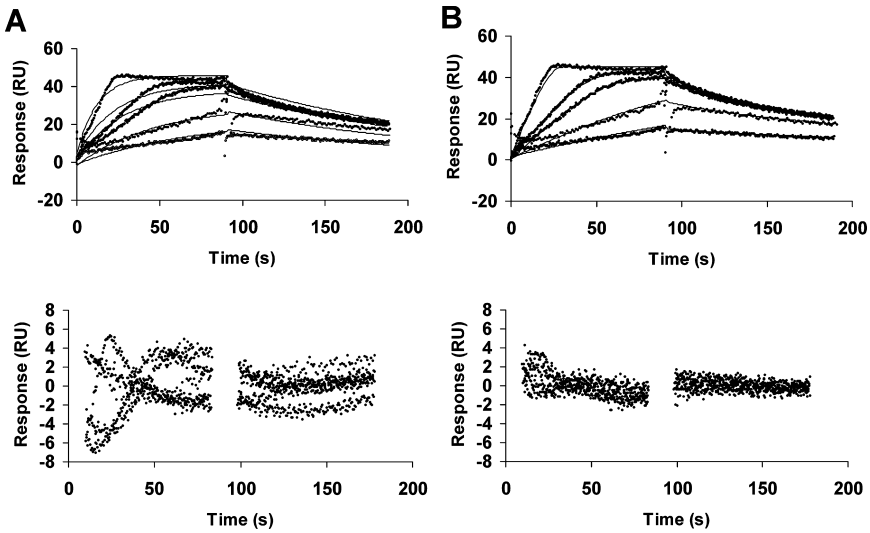

FIGURE 3: Global analysis of SPR biosensor data for AtSPL14 SBP domain protein−DNA interaction kinetic analyses. Top panels: The dotted lines represent SPR sensorgrams (resonance units, RU) obtained by injecting different concentrations of the AtSPL14 SBP domain protein (5, 15, 20, 25, 30, and 50 nM; bottom to top) onto a SA sensor chip coated with a representative 156 bp cognate dsDNA fragment identified by SELEX that bound in EMSA competition assays. Binding data were collected at a flow rate of 75 μL/min. Signals from the control reference cell (coated with a noncognate DNA) were subtracted. Bottom panels: Residual plot showing the difference between measured and calculated responses. (A) Best fits of the binding data to a simple bimolecular 1:1 Langmuir binding model are represented by solid black lines.A residual plot showing the difference between measured and calculated responses indicated that the 1:1 Langmuir binding model is not a good fit (±10 RU). (B) Best fits of the binding data to a simple bimolecular 1:1 mass transfer binding model are represented by solid black lines. A residual plot showing the difference between measured and calculated responses indicated that the 1:1 mass transfer binding model is a good fit (±3 RU). Kinetic binding constants were determined for the mass transfer binding model: the association rate constant $k_a = 2.5 \times 10^7$ M^{-1} s^{-1}, the dissociation rate constant $k_d = 7.4 \times 10^{-2}$ s^{-1}, and the equilibrium binding constant $K_A = k_a/k_d = 3.3 \times 10^8$ M^{-1}.

The final outcome of these analyses was 20 individual sequences. The consensus binding site was identified using the web-based multiple expectation maximization for motif elicitation (MEME) analysis program with manual manipulation to optimize the output and is represented using WebLogo (*36, 37*).

Alignment of the 20 unique sequences indicated CCGTAC(A/G) as the optimal binding site for the AtSPL14 SBP domain (Figure 1). Nucleotides of the core consensus binding motif in a selected individual SBP domain binder (14 in Figure 1A) were mutated to several different nucleotides (Figure 2B). The wild-type (WT) and mutant (M1−M13) DNAs were then tested for binding to FBR6ss in EMSA competition assays. These experiments revealed that the C in position 1 and the A or G in position 7 are dispensable for binding, as dsDNA fragments with mutations in these nucleotides could still effectively compete in EMSA competition assays (Figure 2). Positions 2, 3, and 4 (CGT) are critical for DNA binding, and even conservative changes (i.e., pyrimidine-to-pyrimidine changes in the C and T) effectively abolished the ability of these mutated dsDNAs to compete for binding. Mutation of the A and C in positions 5 and 6 indicated that these nucleotides are also important, as they markedly reduced competition for AtSPL14 SBP domain binding (Figure 2). These mutational analyses support that the AtSPL14 SBP domain recognizes a core consensus binding motif of CGTAC.

AtSPL14 SBP Domain−DNA Interactions by Surface Plasmon Resonance (SPR). SPR analysis was performed using a BIAcore 2000 instrument to measure real-time interactions between DNA coupled to a sensor chip and an analyte (recombinant FBR6ss) in constant flow. A biotin-labeled 156 bp DNA containing the CCGTACA consensus binding motif identified by SELEX (clone 14, Figure 1A) was immobilized to the SA sensor chip. For controls, reference cells were either surface (no immobilized DNA) or noncognate (with a 156 bp random DNA lacking the consensus motif immobilized). The AtSPL14 SBP domain−DNA interactions were then analyzed by SPR.

To determine ideal conditions for kinetic analyses, 15 nM recombinant protein was injected at two different flow rates, 15 and 75 μL/min. We found significant variation with flow rate, suggesting a mass transfer limitation (data not shown). Varying concentrations of recombinant protein (5, 10, 15, 20, 25, 30, and 50 nM) were injected at the higher flow rate (75 μL/min). The SPR response data were then fit to various models using BIAevaluation 3.0 software (Biacore). Nonspecific binding was not observed when the protein concentration was less than 300 nM, and the noncognate DNA reference cell subtraction method was used (Figure S1 of the Supporting Information). The sensorgram data did not fit well to the simple bimolecular 1:1 Langmuir isotherm binding model (Figure 3A) but fit well using the binding with mass transfer model (Figure 3B). According to these data, the AtSPL14 SBP domain has extremely rapid association and dissociation rates with cognate DNA possessing the consensus binding motif; $k_a = 2.5 \times 10^7$ M^{-1} s^{-1} and $k_d = 7.4 \times 10^{-2}$ s^{-1} with equilibrium binding constant $K_A = k_a/k_d = 3.3 \times 10^8$ M^{-1}.

Because of the mass transfer limitation, equilibrium dissociation constants were evaluated by the steady-state binding kinetics (R_{eq}). Nine different protein concentrations were injected at 15 μL/min for 10−15 min to ensure that the binding reaction reached equilibrium. The equilibrium binding constant (K_A) was obtained by fitting the protein concentration corresponding to the steady-state binding level

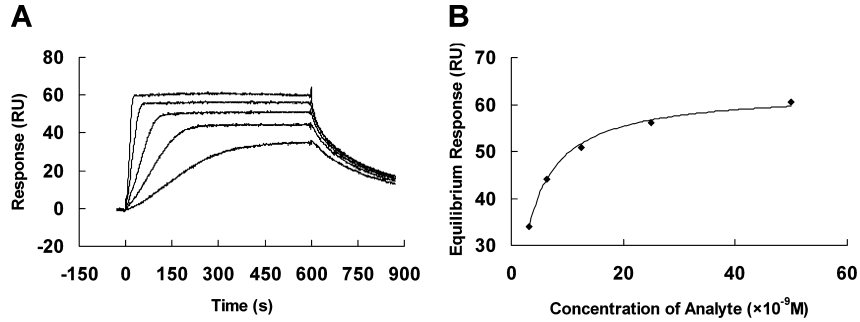

FIGURE 4: Steady-state binding affinity for the AtSPL14 SBP domain protein−DNA interaction. (A) SPR sensorgram of different concentrations of the AtSPL14 SBP domain protein (3.125, 6.25, 12.5, 25, and 50 nM; bottom to top) injected onto a SA sensor chip coated with a representative 156 bp cognate dsDNA fragment identified by SELEX that bound in EMSA competition assays. Binding data were collected at a flow rate of 25 μL/min for 10 min to ensure steady-state equilibrium was reached. The response value at equilibrium (R_{eq}) was calculated from "fitting" straight lines to a chosen section of sensorgrams where the binding response was stabilized (steady state). (B) Plot of the response value (resonance units, RU) at equilibrium (R_{eq}) versus the concentration of analyte. Data were fit to a steady-state affinity model; the equilibrium binding constant $K_A = 3.8 \times 10^8$ M^{-1} and $\chi^2 = 0.758$.

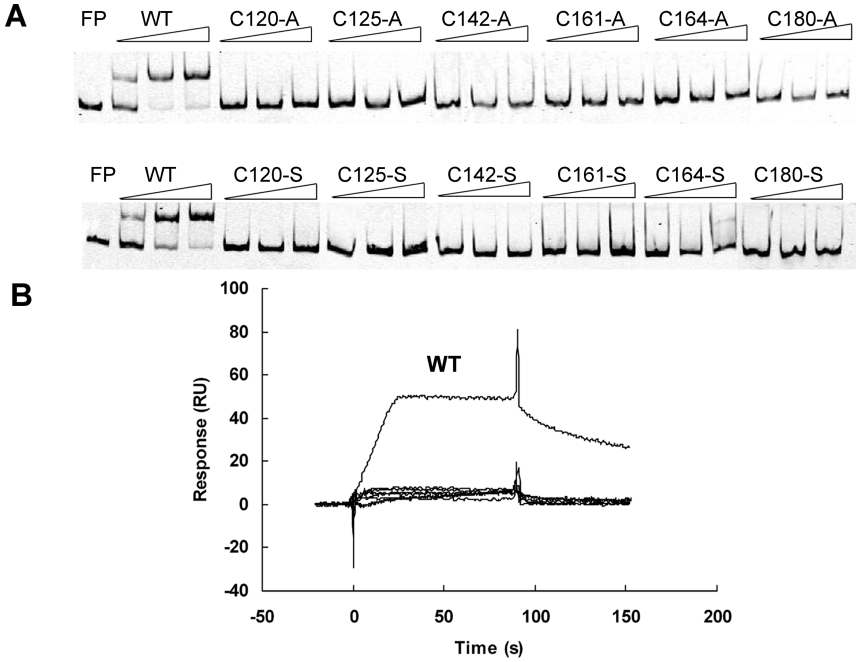

FIGURE 5: Effects of mutating the highly conserved cysteine residues in the AtSPL14 SBP domain on DNA-binding capacity. (A) The ability of wild-type (WT) and mutant (CXXX-A or CXXX-S) AtSPL14 SBP domain proteins to bind to a representative 156 bp cognate dsDNA fragment identified by SELEX was analyzed by electrophoretic mobility shift assays (EMSA). "FP" is free probe (no protein), and triangles represent increasing amounts of proteins in the binding reaction (60, 300, and 600 nM). (B) SPR sensorgrams showing wild-type (WT) AtSPL14 SBP domain protein binding to a cognate dsDNA immobilized on a SA sensor chip (top) compared to the SBP domain mutants (C120-A to C180-A, bottom). Binding data were collected with 50 nM protein injected at a flow rate of 75 μL/min for 90 s.

to a simple 1:1 binding model (Figure 4), resulting in an equilibrium binding constant $K_A = 3.8 \times 10^8$ M^{-1}. Experimental error was determined by performing the experiment in triplicate; $K_A = 3.1 \times 10^8 \pm 1.0 \times 10^8$ M^{-1} (SEM). Therefore, the binding affinities obtained from determining both kinetic rate constants and steady-state equilibrium analyses were similar.

Amino Acids Required for AtSPL14 SBP Domain−DNA Interactions. Multiple sequence alignments of SBP domains from *A. thaliana*, *Antirrhinum majus*, and *C. reinhardtii* indicate that this is a highly conserved protein domain, with sequence identity ranging from 50% to 96% (Figure S2 of the Supporting Information). The consensus sequence is CX_4C-$X_9YX_3HX_2CX_{16}RXCQQCX_3HX_4FDX_4SCRX_2LX_2HNXRR$, where "X" is not absolutely conserved. The six absolutely conserved Cys residues and two of the absolutely conserved His residues have been shown to coordinate two Zn^{2+} ions to form a novel two Zn-finger structure (*26, 27*). The presumed coordinating amino acids of the AtSPL14 SBP domain are shown in Figure S2 of the Supporting Information. To explore whether these six Cys amino acids are required for the AtSPL14 SBP domain to bind DNA, all six amino acids were individually mutated to Ala and Ser, and the mutant proteins were assayed for DNA-binding efficiency by EMSA. All 12 Cys substitutions almost completely abolished the ability of the AtSPL14 SBP domain to bind DNA, with the exception of C164-A and C164-S, which exhibited very weak binding at high protein concentrations (Figure 5). We also tested the ability of the mutant proteins to bind DNA by SPR. The binding of the mutant AtSPL14 SBP domain proteins was markedly reduced compared to the wild-type protein (Figure 5). Therefore, all six highly conserved Cys amino acids are important for DNA binding, but weak affinity is retained when one of the Cys amino

acids predicted to coordinate a Zn^{2+} ion in the second Zn-finger structure is mutated.

DISCUSSION

Our interest in determining the AtSPL14 SBP domain DNA-binding motif and binding kinetics derives from identification of an *A. thaliana* mutant with a disruption in the *AtSPL14* gene (At1g20980). The *A. thaliana* FB1-resistant (*fbr6*) mutant was originally identified by selecting for mutants capable of growth and development on media containing the fungal toxin fumonisin B1 (FB1). FB1 disrupts sphingolipid metabolism in eukaryotes (*38*) and induces PCD, dependent on transcription, translation, reversible protein phosphorylation, light, and hormone signaling pathways in *A. thaliana* (*10, 11*). In addition to resistance to FB1, the *fbr6* mutant also exhibits altered plant architecture, including elongated petioles and enhanced leaf margin serration (*9*). Knowledge of the AtSPL14 DNA-binding site (and potentially regulated genes) is critical to fully understanding the physiological functions of this sequence-specific DNA-binding transcription factor.

The AtSPL14 SBP Domain Binds to the Core GTAC Consensus Target Site but Requires an Additional Flanking Nucleotide for Effective Interaction. AtSPL14 (At1g20980) encodes a 1035 amino acid–protein with an SBP DNA-binding domain (http://srs.ebi.ac.uk; IPR004333), a bipartite nuclear localization signal (aa 117–193), and ankyrin repeats that mediate protein–protein interactions (IPR002110; aa 821–941) in the C-terminal region of the protein (*9, 13, 39, 40*). The highly conserved SBP DNA-binding domain is a Cys- and His-rich region (consensus: $CX_4CX_{13}HX_5HX_{15}CQQCX_3HX_{11}C$) found only in proteins from photosynthetic organisms (*12, 13, 18, 28*). The founding members of the SBP domain gene family (SBP1 and SBP2 from *A. majus*) were identified by their ability to bind to the upstream regulatory region of the *SQUAMOSA* floral meristem identity gene (*29*). Previous reports indicated that *A. majus* proteins and some *A. thaliana* SBP domain proteins bind DNA encompassing a ten nucleotide motif common to *cis* regulatory elements in the orthologous *A. majus SQUAMOSA* and *A. thaliana APETALA1* gene promoters and a similar motif in the *A. majus DEFH84* promoter *in vitro* (*13, 17*). Alignment of these sequences revealed a putative consensus DNA-binding motif of TNCGTACAA (*13*). It appears that GTAC is the core DNA-binding motif for all SBP domains described so far, but nucleotides flanking the core motif are preferred by different SBP domain proteins.

We used a completely random approach, referred to as systematic evolution of ligands by exponential enrichment (SELEX) or random binding site selection (RBSS), to identify the consensus DNA-binding site for AtSPL14. These analyses revealed CCGTAC(A/G) as the optimal binding site for the AtSPL14 SBP domain (Figure 1). We found no evidence for a palindromic binding motif, which would suggest that binding occurs as a dimer, consistent with a previous report that other SBP domains bind DNA with a 1:1 stoichiometry (*26*). To verify the importance of the consensus motif, we mutated the individual nucleotides of the predicted binding site CCGTAC(A/G) to obtain both conserved and nonconserved substitutions of each base except the 3′-end A/G (Figure 2B). Mutations in the CGTAC core markedly reduced competition for AtSPL14 binding, but the C at the 5′-end and the A/G at the 3′-end were dispensable (Figure 2). Therefore, each individual nucleotide of the core motif CGTAC is necessary for effective AtSPL14 SBP domain DNA binding (Figure 2).

Birkenbihl et al. (*28*) recently used a similar random binding site selection with G and T fixed at positions 7 and 8 (of 16 total "random" nucleotides) to identify binding sites for AtSPL3 and AtSPL8 SBP domains. A high preference for at least one more C at the 5′-end of the core consensus GTAC motif was found for AtSPL3 (83%), but not for AtSPL8. Therefore, the recognition site we determined for AtSPL14 is more similar to that of AtSPL3 than AtSPL8. The preference for a C flanking the GTAC core must be due to a specific amino acid−nucleotide interaction. The overall sequence identities between the AtSPL14 SBP domain and those of AtSPL3 (70%) and AtSPL8 (74%) are quite similar (Figure S2 of the Supporting Information), with only three amino acid differences in the Zn2 region proposed to interact directly with DNA (*27*). AtSPL14 and AtSPL3 have a Glu, Arg, and Gly whereas AtSPL8 has Asn, Lys, and Asp, respectively (Figure S2 of the Supporting Information). Whereas no simple universal code has been elucidated, specificity is imparted in most protein−DNA contacts by hydrogen bonding in the major groove (*41*). Statistical analysis of atomic interactions in 139 protein−DNA complexes analyzed from the Protein Data Bank (PDB) revealed favored amino acid−nucleotide pairs (*42*). The authors categorized direct amino acid−nucleotide contacts, including hydrogen bonds and electrostatic, hydrophobic, and other van der Waals interactions. Whereas contacts with the sugars or phosphates of DNA contribute to DNA–protein stability, only H-bonds to nucleotide bases can confer sequence specificity. In interactions with nucleotide bases, the most commonly observed interaction was Arg with G (*42*). Therefore, it seems most likely that the substitution of Lys in AtSPL8 for Arg in AtSPL14 and AtSPL3 renders the 5′ nucleotide flanking the core GTAC motif unimportant. This hypothesis will need to be tested experimentally.

Simple pattern matching searches for the consensus binding sequence reported for the *A. majus* SBP proteins "TNCGTACAA" (*13, 29*) upstream of annotated *A. thaliana* genes identified 331 and 640 putative *SPL*-regulated genes with the pattern within 500 and 1000 base pairs of the translation start site, respectively. Using the consensus DNA-binding motif, we identified for AtSPL14 (CGTAC) more than 6000 genes with the motif within 500 base pairs of the translation start site as possible AtSPL14 targets, and one gene of unknown function has 16 occurrences. Combined with microarray gene expression data comparing the transcriptomes of the *fbr6* mutant to wild-type plants, a subset of candidate target genes for AtSPL14 were identified (data not shown). Whereas some of these promoter sequences also bind to AtSPL14 *in vitro*, additional experiments, such as chromatin immunoprecipitation (ChIP), will be required to verify that these are true targets for AtSPL14 *in vivo*.

The Kinetic Binding Parameters of SBP Domains Differ. The SBP domain DNA binding is dependent on the presence of Zn^{2+} ions (*18, 28*). The NMR-resolved structures of SBP domains revealed that the SBP domain forms a novel two Zn structure DNA-binding domain (*26*). The two Zn^{2+} ions are coordinated by three Cys residues and one His residue,

forming two Zn structures in CCCH (Zn1) and CCHC (Zn2) configurations (Figure S2 of the Supporting Information). We mutated all six highly conserved Cys to Ala and Ser and determined the SBP−DNA binding efficiency by EMSA and SPR. All 12 mutations markedly reduced the AtSPL14−DNA interaction (Figure 2), verifying that all six conserved Cys in the AtSPL14 SBP DNA-binding domain are important for AtSPL14 protein−DNA interaction and consistent with the supposition that these Cys residues participate in Zn^{2+} ion binding (*26, 28*). However, the C164-A and C164-S (corresponding to the second Cys in Zn2) mutant proteins retained some weak binding ability (Figures 2 and S2 of the Supporting Information). The second Cys and the His in Zn1 and the first and fourth Cys in Zn2 were reported to be critical for AtSPL1 DNA binding (*28*). In that study the second Cys in Zn2 was not mutated, but the His in Zn2 was found to be somewhat dispensable (*28*). Therefore, we independently determined that all of the Zn1 coordinating residues are essential, but two of the presumed Zn2 coordinating residues (the His and second Cys) are not absolutely required for SBP domain DNA binding. These findings support the conclusions derived from the NMR structure of a truncated SBP domain protein (AtSPL12). The Zn1 structure is critical for overall structure, and removal of part of the Zn2 domain affected DNA binding but had little effect on overall folding (*27*). It is not yet clear whether proteins with mutations of the Zn^{2+} ion coordinating amino acids (His and second Cys) in the Zn2 structure can still bind a second Zn^{2+} ion. Another His residue is absolutely conserved in SBP domains (His187 in AtSPL14, Figure S2 of the Supporting Information) and might serve as a substitute fourth ligand. Alternatively, acidic residues or a water molecule might serve as the fourth coordinating ligand (*43*).

The AtSPL14 DNA-binding kinetics was analyzed by surface plasmon resonance (SPR). The mass transfer limitation due to the rapid association ($>10^7$) and dissociation rates ($>10^{-2}$) made determination of reliable kinetic constants difficult using conventional SPR (*32*). Therefore, we also evaluated steady-state binding at equilibrium. The determined equilibrium binding constant, K_A (3.8×10^8 M^{-1}), is similar to the reported values (9.6×10^7 M^{-1} and $>5 \times 10^8$ M^{-1}) for the AtSPL4 and AtSPL12 SBP domains, respectively, and 1 order of magnitude greater than the value (2.8×10^7 M^{-1}) reported for the AtSPL7 SBP domain (*26, 27*). Kinetic rate constants were not reported for other SBP domain proteins.

The different K_A values determined for different SBP domains might be due to the different salt concentrations in the analyte. Our data were generated in HBS−EP buffer (containing 150 mM NaCl), whereas the K_A of binding for AtSPL4, AtSPL7, and AtSPL12 was assayed in the presence of 100 or 300 mM KCl. The K_A for AtSPL12 and AtSPL4 at 100 mM KCl ($>5 \times 10^8$ M^{-1} and 2.8×10^7 M^{-1}, respectively) was higher than those determined at 300 mM KCl (3.2×10^7 M^{-1} and 2.1×10^6 M^{-1}, respectively), suggesting that salt concentration affects SBP domain−DNA-binding affinity. Therefore, electrostatic forces contribute to the SBP−DNA interaction, as was also observed in other protein−DNA interactions (*44, 45*).

Conclusions. In summary, different SBP domain proteins display different binding affinities to the same DNA and different selectivity for DNA targets. Even though they contain the same core consensus binding motif (GTAC), the *A. thaliana APETALA1* gene-derived DNA and DNA containing the *C. reinhardtii* copper-responsive element (CuRE) had different affinities for several SBP domain proteins (*28*). Our results revealed that AtSPL14−DNA binding is highly sequence selective and allow us to hypothesize which particular amino acids may confer that specificity. Moreover, the well-conserved SBP domains possess diverse DNA-binding affinities for similar DNA sequences. These observations will be useful, in conjunction with additional experimentation, to identify the gene targets for individual SBP domain family members to understand their physiological functions in the context of whole organisms.

ACKNOWLEDGMENT

We thank Weimin Zhang for technical assistance with the SPR experiments, Michael Fromm, Director of the University of Nebraska−Lincoln Center for Biotechnology, for access to the Biacore 2000 and funding for Biacore training, Dmitri Fomenko for help with the MEME analyses, and other members of the Stone laboratory for useful discussions.

SUPPORTING INFORMATION AVAILABLE

SPR data analysis comparing the subtraction of the signals from a blank reference cell and a reference cell coated with a noncognate DNA indicates that subtracting data from a reference cell coated with noncognate DNA is the preferred control (Figure S1). An amino acid alignment of the SBP DNA-binding domains encoded by the 16 *A. thaliana* genes, the 2 *A. majus* genes, and the CuRE-binding *C. reinhardtii* gene is provided with a schematic of the Zn^{2+} ion coordinating residues (Figure S2). The oligonucleotide primers used for site-directed mutagenesis of both the DNA target and the AtSPL14 SBP domain protein are shown in supplementary tables (Tables S1 and S2). This material is available free of charge via the Internet at http://pubs.acs.org.

REFERENCES

1. Deyhle, F., Sarkar, A. K., Tucker, E. J., and Laux, T. (2007) WUSCHEL regulates cell differentiation during anther development. *Dev. Biol. 302*, 154–159.
2. van Doorn, W. G., and Woltering, E. J. (2005) Many ways to exit? Cell death categories in plants. *Trends Plant Sci. 10*, 117–122.
3. Groover, A., and Jones, A. M. (1999) Tracheary element differentiation uses a novel mechanism coordinating programmed cell death and secondary cell wall synthesis. *Plant Physiol. 119*, 375–384.
4. Demura, T., Tashiro, G., Horiguchi, G., Kishimoto, N., Kubo, M., Matsuoka, N., Minami, A., Nagata-Hiwatashi, M., Nakamura, K., Okamura, Y., Sassa, N., Suzuki, S., Yazaki, J., Kikuchi, S., and Fukuda, H. (2002) Visualization by comprehensive microarray analysis of gene expression programs during transdifferentiation of mesophyll cells into xylem cells. *Proc. Natl. Acad. Sci. U.S.A. 99*, 15794–15799.
5. Fukuda, H. (2000) Programmed cell death of tracheary elements as a paradigm in plants. *Plant Mol. Biol. 44*, 245–253.
6. Gechev, T. S., Van Breusegem, F., Stone, J. M., Denev, I., and Laloi, C. (2006) Reactive oxygen species as signals that modulate plant stress responses and programmed cell death. *BioEssays 28*, 1091–1101.
7. Gilchrist, D. G. (1998) Programmed cell death in plant disease: the purpose and promise of cellular suicide. *Annu. Rev. Phytopathol. 36*, 393–414.
8. Beers, E. P., and McDowell, J. M. (2001) Regulation and execution of programmed cell death in response to pathogens, stress and developmental cues. *Curr. Opin. Plant Biol. 4*, 561–567.

9. Stone, J. M., Liang, X., Nekl, E. R., and Stiers, J. J. (2005) *Arabidopsis* AtSPL14, a plant-specific SBP-domain transcription factor, participates in plant development and sensitivity to fumonisin B1. *Plant J. 41*, 744–754.
10. Stone, J. M., Heard, J. E., Asai, T., and Ausubel, F. M. (2000) Simulation of fungal-mediated cell death by fumonisin B1 and selection of fumonisin B1-resistant (*fbr*) *Arabidopsis* mutants. *Plant Cell 12*, 1811–1822.
11. Asai, T., Stone, J. M., Heard, J. E., Kovtun, Y., Yorgey, P., Sheen, J., and Ausubel, F. M. (2000) Fumonisin B1-induced cell death in *Arabidopsis* protoplasts requires jasmonate-, ethylene-, and salicylate-dependent signaling pathways. *Plant Cell 12*, 1823–1836.
12. Xie, K., Wu, C., and Xiong, L. (2006) Genomic organization, differential expression and interaction of SQUAMOSA promoter-binding-like transcription factors and microRNA156 in rice. *Plant Physiol. 142*, 280–293.
13. Cardon, G., Hohmann, S., Klein, J., Nettesheim, K., Saedler, H., and Huijser, P. (1999) Molecular characterisation of the *Arabidopsis* SBP-box genes. *Gene 237*, 91–104.
14. Moreno, M. A., Harper, L. C., Krueger, R. W., Dellaporta, S. L., and Freeling, M. (1997) *liguleless1* encodes a nuclear-localized protein required for induction of ligules and auricles during maize leaf organogenesis. *Genes Dev. 11*, 616–628.
15. Wang, H., Nussbaum-Wagler, T., Li, B., Zhao, Q., Vigouroux, Y., Faller, M., Bomblies, K., Lukens, L., and Doebley, J. F. (2005) The origin of the naked grains of maize. *Nature 436*, 714–719.
16. Unte, U. S., Sorensen, A. M., Pesaresi, P., Gandikota, M., Leister, D., Saedler, H., and Huijser, P. (2003) SPL8, an SBP-box gene that affects pollen sac development in *Arabidopsis*. *Plant Cell 15*, 1009–1019.
17. Cardon, G. H., Hohmann, S., Nettesheim, K., Saedler, H., and Huijser, P. (1997) Functional analysis of the *Arabidopsis thaliana* SBP-box gene SPL3: a novel gene involved in the floral transition. *Plant J. 12*, 367–377.
18. Kropat, J., Tottey, S., Birkenbihl, R. P., Depege, N., Huijser, P., and Merchant, S. (2005) A regulator of nutritional copper signaling in *Chlamydomonas* is an SBP domain protein that recognizes the GTAC core of copper response element. *Proc. Natl. Acad. Sci. U.S.A. 102*, 18730–18735.
19. Merchant, S. S., Allen, M. D., Kropat, J., Moseley, J. L., Long, J. C., Tottey, S., and Terauchi, A. M. (2006) Between a rock and a hard place: trace element nutrition in *Chlamydomonas*. *Biochim. Biophys. Acta 1763*, 578–594.
20. Zhang, Y., Schwarz, S., Saedler, H., and Huijser, P. (2007) SPL8, a local regulator in a subset of gibberellin-mediated developmental processes in *Arabidopsis*. *Plant Mol. Biol. 63*, 429–439.
21. Manning, K., Tor, M., Poole, M., Hong, Y., Thompson, A. J., King, G. J., Giovannoni, J. J., and Seymour, G. B. (2006) A naturally occurring epigenetic mutation in a gene encoding an SBP-box transcription factor inhibits tomato fruit ripening. *Nat. Genet. 38*, 948–952.
22. Lee, J., Park, J. J., Kim, S. L., Yim, J., and An, G. (2007) Mutations in the rice *liguleless* gene result in a complete loss of the auricle, ligule, and laminar joint. *Plant Mol. Biol. 65*, 487–499.
23. Jones-Rhoades, M. W., and Bartel, D. P. (2004) Computational identification of plant microRNAs and their targets, including a stress-induced miRNA. *Mol. Cell 14*, 787–799.
24. Xie, Z., Allen, E., Fahlgren, N., Calamar, A., Givan, S. A., and Carrington, J. C. (2005) Expression of *Arabidopsis* MIRNA genes. *Plant Physiol. 138*, 2145–2154.
25. Gandikota, M., Birkenbihl, R. P., Hohmann, S., Cardon, G. H., Saedler, H., and Huijser, P. (2007) The miRNA156/157 recognition element in the 3′ UTR of the Arabidopsis SBP box gene SPL3 prevents early flowering by translational inhibition in seedlings. *Plant J. 49*, 683–693.
26. Yamasaki, K., Kigawa, T., Inoue, M., Tateno, M., Yamasaki, T., Yabuki, T., Aoki, M., Seki, E., Matsuda, T., Nunokawa, E., Ishizuka, Y., Terada, T., Shirouzu, M., Osanai, T., Tanaka, A., Seki, M., Shinozaki, K., and Yokoyama, S. (2004) A novel zinc-binding motif revealed by solution structures of DNA-binding domains of *Arabidopsis* SBP-family transcription factors. *J. Mol. Biol. 337*, 49–63.
27. Yamasaki, K., Kigawa, T., Inoue, M., Yamasaki, T., Yabuki, T., Aoki, M., Seki, E., Matsuda, T., Tomo, Y., Terada, T., Shirouzu, M., Tanaka, A., Seki, M., Shinozaki, K., and Yokoyama, S. (2006) An *Arabidopsis* SBP-domain fragment with a disrupted C-terminal zinc-binding site retains its tertiary structure. *FEBS Lett. 580*, 2109–2116.
28. Birkenbihl, R. P., Jach, G., Saedler, H., and Huijser, P. (2005) Functional dissection of the plant-specific SBP-domain: overlap of the DNA-binding and nuclear localization domains. *J. Mol. Biol. 352*, 585–596.
29. Klein, J., Saedler, H., and Huijser, P. (1996) A new family of DNA binding proteins includes putative transcriptional regulators of the *Antirrhinum majus* floral meristem identity gene SQUAMOSA. *Mol. Gen. Genet. 250*, 7–16.
30. Sambrook, J., and Russell, D. W. (2001) *Molecular cloning: a laboratory manual*, 3rd ed., Cold Spring Harbor Laboratory Press, Cold Spring Harbor, NY.
31. Watson, D. K., Kitching, R., Vary, C., Kola, I., and Seth, A. (2000) Isolation of target gene promoter/enhancer sequences by whole genome PCR method, in *Transcription Factor Protocols* (Tymms, M. J., Ed.) pp 1–11, Humana Press, Totowa, NJ.
32. Karlsson, R. (1999) Affinity analysis of non-steady-state data obtained under mass transport limited conditions using BIAcore technology. *J. Mol. Recognit. 12*, 285–292.
33. Kalifa, Y., Gilad, A., Konrad, Z., Zaccai, M., Scolnik, P. A., and Bar-Zvi, D. (2004) The water- and salt-stress-regulated *Asr1* (abscisic acid stress ripening) gene encodes a zinc-dependent DNA-binding protein. *Biochem. J. 381*, 373–378.
34. Manuel, M., Rallu, M., Loones, M. T., Zimarino, V., Mezger, V., and Morange, M. (2002) Determination of the consensus binding sequence for the purified embryonic heat shock factor 2. *Eur. J. Biochem. 269*, 2527–2537.
35. Ausubel, F. M., Brent, R., Kingston, R. E., Moore, D. D., Seidman, J. G., Smith, J. A., and Struhl, K., Eds. (2006) *Current Protocols in Molecular Biology*, John Wiley and Sons, New York, NY.
36. Grundy, W. N., Bailey, T. L., Elkan, C. P., and Baker, M. E. (1997) Meta-MEME: motif-based hidden Markov models of protein families. *Comput. Appl. Biosci. 13*, 397–406.
37. Crooks, G. E., Hon, G., Chandonia, J. M., and Brenner, S. E. (2004) WebLogo: a sequence logo generator. *Genome Res. 14*, 1188–1190.
38. Desai, K., Sullards, M. C., Allegood, J., Wang, E., Schmelz, E. M., Hartl, M., Humpf, H. U., Liotta, D. C., Peng, Q., and Merrill, A. H., Jr. (2002) Fumonisins and fumonisin analogs as inhibitors of ceramide synthase and inducers of apoptosis. *Biochim. Biophys. Acta 1585*, 188–192.
39. Chen, L. (1999) Combinatorial gene regulation by eukaryotic transcription factors. *Curr. Opin. Struct. Biol. 9*, 48–55.
40. Robbins, J., Dilworth, S. M., Laskey, R. A., and Dingwall, C. (1991) Two interdependent basic domains in nucleoplasmin nuclear targeting sequence: identification of a class of bipartite nuclear targeting sequence. *Cell 64*, 615–623.
41. Luscombe, N. M., Laskowski, R. A., and Thornton, J. M. (2001) Amino acid-base interactions: a three-dimensional analysis of protein-DNA interactions at an atomic level. *Nucleic Acids Res. 29*, 2860–2874.
42. Lejeune, D., Delsaux, N., Charloteaux, B., Thomas, A., and Brasseur, R. (2005) Protein-nucleic acid recognition: statistical analysis of atomic interactions and influence of DNA structure. *Proteins 61*, 258–271.
43. Kornhaber, G. J., Snyder, D., Moseley, H. N., and Montelione, G. T. (2006) Identification of zinc-ligated cysteine residues based on $^{13}C\alpha$ and $^{13}C\beta$ chemical shift data. *J. Biomol. NMR 34*, 259–269.
44. Seimiya, M., and Kurosawa, Y. (1996) Kinetics of binding of Antp homeodomain to DNA analyzed by measurements of surface plasmon resonance. *FEBS Lett. 398*, 279–284.
45. Oda, M., Furukawa, K., Sarai, A., and Nakamura, H. (1999) Kinetic analysis of DNA binding by the c-Myb DNA-binding domain using surface plasmon resonance. *FEBS Lett. 454*, 288–292.

BI701431Y